JOURNAL OF SOLID STATE CHEMISTRY 66, 86–94 (1987)

Crystal Structure of a New Lamellar Compound: $Ag_{1/2}In_{1/2}PS_3$

Z. OUILI, A. LEBLANC, AND P. COLOMBET*

Laboratoire de Chimie des Solides, U.A. 279, 2, rue de la Houssinière, 44072 Nantes Cedex, France

Received February 19, 1986; in revised form April 21, 1986

The lamellar compound $Ag_{1/2}In_{1/2}PS_3$ was synthesized from the elements, except for In which was introduced through In_2S_3, and heated in evacuated silica tubes for 1 week at 700°C. Its crystal structure has been solved from 820 independent reflections and 18 parameters, the least-squares refinement yielding $R = 0.028$. The crystal symmetry is trigonal, space group $P\bar{3}1c$, with lattice constants $a = 6.182(2)$ Å, $c = 12.957(2)$ Å, $V = 428.8(4)$ Å^3, and $Z = 4$. The structure is built up with S[$Ag_{1/3}In_{1/3}(P_2)_{1/3}$]S slabs with an AB-type sulfur sequence. All the cations are distributed orderly in the $a-b$ planes, each of them forming a triangular lattice. The structural features of the studied compound and those of the MPX_3 (M = transition metal; X = S, Se) are compared. In particular, the silver thermal factor is found to be by far the largest (4.2 Å^2) and to be very anisotropic. In addition, the driving force for the ordered distribution nature of the cations in the $M(I)_{1/2}M(III)_{1/2}PS_3$ materials is discussed, together with the origin and nature of the cuts in the magnetic zigzagging chains in $Ag_{1/2}Cr_{1/2}PS_3$.

1. Introduction

The two-dimensional MPX_3 (M = first-row transition metal; X = S, Se) series has been the subject of great interest because of its potential use in high-energy density lithium batteries (*1, 2*). In addition to its practical importance, the MPX_3 family provides an important model for studying the consequences of ordered substitutions, as far as the magnetic properties are concerned (*3, 4*). In the case of sulfides, the divalent metal M(II) could effectively be replaced by a couple of mono- and trivalent metals ($\frac{1}{2}M(I) + \frac{1}{2}M(III)$), where M(III) = Cr and M(I) = Cu (*3*) or Ag (*4*), without considerable change in the whole crystallographic features but for the following aspects:

1. From quasi-two (honeycomb lattice) in $MnPX_3$, $FePX_3$, and $NiPX_3$ (X = S, Se) (*5*), the magnetic network dimensionality shifts to nearly 3 in the copper-containing compound (*3*), whereas it shifts to quasi-one in the silver-containing one (*4, 6*). In $Cu_{1/2}Cr_{1/2}PS_3$, chromium(III) ions form a weakly ferromagnetic planar triangular lattice. In $Ag_{1/2}Cr_{1/2}PS_3$, they form strongly antiferromagnetic zigzagging chains.

2. As for the monovalent element, the single-crystal X-ray diffraction studies showed that it is characterized by a tendency to be displaced from the center of the octahedral site toward its triangular faces, especially in the case of the Cu-containing compound. It has then been suggested that such a characteristic denotes a preference for M(I) to be 3- rather than 6-coordinated in these MPX_3-derived materials (*4*). In

* To whom correspondence should be addressed.

0022-4596/87 $3.00

fact, a recent EXAFS investigation of $Cu_{1/2}Cr_{1/2}PS_3$ has led to the conclusion that this compound presents, on the Cu sublattice, a disordered distribution of vacancies with bimetallic [S_3Cu . . . CuS_3] and monometallic [CuS_6] entities (*7*). To the contrary, the silver–silver bimetallic entities do not exist in the Ag-containing compound (*8*).

In addition to the above points, and as far as the Ag-containing compound is concerned, the 1D magnetic properties have been shown to be greatly affected by irradiation- and substitution-induced disorders (*9*). In particular, the observed magnetic behavior of the $Ag_{1/2}Cr_{(1/2-x)}In_xPS_3$ system suggests that, for $x \lesssim 0.20$, these compounds are spin glasses at lower temperatures and that the magnetic interactions are predominantly AF (*9, 10*): the nn coupling has approximately the same value as in the nonsubstituted compound and is predominant as compared to more distant interactions. For $x \gtrsim 0.35$, the nn intraplanar coupling is weakly ferromagnetic, which has been assumed to result from a new *M*(I)–*M*(III) distribution nature (*10*). Preliminary powder X-ray spectra analyses indicate that the chromium-substituted compounds corresponding to $x \lesssim 0.20$ are structurally similar to $Ag_{1/2}Cr_{1/2}PS_3$; i.e., the Cr(III) sublattice consists of broken chains, in agreement with the susceptibility measurements (*9, 10*). For $0.35 \lesssim x \lesssim 0.50$, the powder X-ray spectra were indexed assuming an orthorhombic cell, and, from systematic absences, the space group was determined as being $P2_122_1$. For $x = 0.50$, the cell parameters were found to be (*10*) $a = 6.186(1)$ Å, $b = 10.673(3)$ Å, $c = 12.960(2)$ Å. Consistent with the similarity of the magnetic behaviors of $Ag_{1/2}Cr_{0.10}In_{0.40}PS_3$ and $Cu_{1/2}Cr_{1/2}PS_3$, the (Cr, In) sublattice was proposed to be triangular. A two-phase domain ranges from $x \simeq 0.20$ to $\simeq 0.35$.

This work is focused essentially on a single-crystal X-ray diffraction study of $Ag_{1/2}In_{1/2}PS_3$ ($x = 0.50$). It was undertaken with the aim of checking our previous structural assumptions concerning the orthorhombic $x \gtrsim 0.35$ phase (*10*), in particular, the triangular nature of the *M*(III) arrangement. The driving force for the *M*(I)–*M*(III) ordered distribution geometry in this series of materials is discussed. It is also shown that the here reported structural results shed some light on the nature of the chain defects for the monoclinic $0 \lesssim x \lesssim 0.20$ phase, which is the most interesting one from the magnetic point of view, and for which no single crystal was obtained so far for X-ray study, but for $x = 0$.

2. Experimental

The synthetic procedure has been described elsewhere (*9, 10*). All the elements were purchased from Koch Light Corporation (Ag > 99.99%; S > 99.9%; In,P > 99%). No transport agent was used and the ochre single crystals grow within the powder. The photographs examined in Buerger and Weissenberg cameras show the Laue symmetry to be $\bar{3}m$, in contrast to what was previously reported on the basis of the systematic extinctions deduced from powder data (*10*). The conditions limiting possible reflections on the (*hkl*) planes, *hhl* with $l = 2n$, correspond to the $P\bar{3}1c$ space group. The powder data were thus reexamined. Effectively, the spectra can also be satisfactorily indexed according to a hexagonal cell. The room-temperature cell parameter values for the powder sample, least-squares refined using a Guinier–Nonius FR552 powder diffractometer (Si standard, Cu$K\alpha_1$ radiation), are $a = b = 6.182(2)$ Å, $c = 12.957(2)$ Å, $\gamma = 120°$. As compared to the previously assumed orthorhombic cell parameters (see Introduction), *a* and *c* are unchanged and the new *b* parameter is related to the previous one by the relation $b_{hex} = b_{orth}/\sqrt{3}$. Hence, the number of formula units per unit hexagonal cell is $Z = 4$ ($Z = 8$

TABLE I

OBSERVED AND CALCULATED POWDER DATA (THE INTENSITIES ARE DETERMINED USING THE LAZY PULVERIX PROGRAM) FOR $Ag_{1/2}In_{1/2}PS_3$ ($x = 0.50$)

d_{obs} (Å)	d_{calcd} (Å)	$h\,k\,l$	$100\,I/I_0$	d_{obs} (Å)	d_{calcd} (Å)	$h\,k\,l$	$100\,I/I_0$
6.481	6.479	0 0 2	94.4	1.8323	1.8324	2 1 3	1.6
5.355	5.354	1 0 0	2.9			2 1 $\bar{3}$	0.4
4.951	4.950	1 0 1	2.5	1.7838	1.7845	3 0 0	27.5
4.129	4.127	1 0 2	3.5	1.7690	1.7702	1 1 6	11.0
3.367	3.361	1 0 3	10.9			1 1 $\bar{6}$	0.1
3.090	3.091	1 1 0	25.4		1.7678	3 0 1	0.0
2.793	2.789	1 1 2	4.5	1.7202	1.7205	3 0 2	6.2
		1 1 $\bar{2}$	100.0	1.6195	1.6196	0 0 8	4.4
2.621	2.621	2 0 1	2.0	1.5944	1.5949	2 1 5	0.7
2.476	2.4739	2 0 2	1.2			2 1 $\bar{5}$	2.2
2.3319	2.3325	1 0 5	6.7	1.5452	1.5455	2 2 0	2.8
2.2747	2.2752	2 0 3	1.1	1.5032	1.5023	2 2 2	11.6
2.2368	2.2362	1 1 4	25.1	1.4761	1.4766	2 1 6	1.0
		1 1 $\bar{4}$	18.3			2 1 $\bar{6}$	0.8
2.1599	2.1595	0 0 6	3.1	1.4473	1.4473	3 1 2	0.5
2.0224	2.0235	2 1 0	0.4			3 1 $\bar{2}$	0.2
1.9985	1.9993	2 1 1	1.0	1.4053	1.4042	3 1 3	0.3
		2 1 $\bar{1}$	0.0			3 1 $\bar{3}$	1.1
1.8622	1.8619	2 0 5	1.8	1.3946	1.3949	2 2 4	3.2
						2 2 $\bar{4}$	4.4

for the orthorhombic one). The calculated and observed d-spacings are given in Table I, as well as the calculated intensities as obtained using the Lazy Pulverix Program (*11*).

For the purpose of comparison with the results given in (*10*), we then reindexed the powder data for $Ag_{1/2}In_{0.40}Cr_{0.10}PS_3$, which belongs to the previously assumed orthorhombic phase, by considering a hexagonal cell (Table II), and we found $a = b = 6.157$ Å, $c = 12.954$ Å, $\gamma = 120°$.

$Ag_{1/2}In_{1/2}PS_3$ single-crystal X-ray data were collected from a crystal of the dimensions $0.05 \times 0.07 \times 0.07$ mm^3 with an automated four-circle diffractometer (ENRAF–NONIUS) working with a graphite monochromated Mo$K\alpha$ radiation. The 7800 reflections within one quarter of the reciprocal plane were recorded in the angle range 1–40° (scan angle: $1 + 0.35 \tan \theta$). The absorption factor is $\mu = 65.5$ cm^{-1} and no correction was made for the absorption. The intensities were corrected for the Lorentz and polarization factors. After the reflections with $I < 4\sigma(I)$ were omitted and equivalent F values averaged, a total of 820 reflections were utilized for the refinement. No unobserved reflections were detected and no bad data were rejected.

3. Structure Refinement

The structural parameters were refined by the least-squares techniques using the programs belonging to the SDS–PLUS package. The hexagonal unit cell parameters of $Ag_{1/2}In_{1/2}PS_3$ (a, b, c) are related to those of monoclinic $Cu_{1/2}Cr_{1/2}PS_3$ (a', b', c', β') (*3*) by $a \simeq a'$, $b \simeq b'/\sqrt{3}$, and $c \simeq c' \sin \beta'$. On the basis of, first, the c value (~13 Å), and second, the fact that c is perpendicular to the a–b plane, the calculations were performed assuming a sulfur stacking of the (AB) type, with two AB layers per unit cell (Fig. 1), rather than of the (ABC) type as found in the $M_{1/2}Cr_{1/2}PS_3$ (M = Ag, Cu) materials. We also took into account the possible triangular nature of the In sublattice, as

TABLE II

OBSERVED AND CALCULATED POWDER DATA (THE INTENSITIES ARE DETERMINED USING THE LAZY PULVERIX PROGRAM) FOR $Ag_{1/2}In_{0.40}Cr_{0.10}PS_3$ ($x = 0.40$)

d_{obs} (Å)	d_{calcd} (Å)	$h\,k\,l$	$100\,I/I_0$	d_{obs} (Å)	d_{calcd} (Å)	$h\,k\,l$	$100\,I/I_0$
6.467	6.477	0 0 2	91.6	1.8267	1.8264	2 1 3	1.7
5.320	5.332	1 0 0	1.1			2 1 $\bar{3}$	0.4
4.924	4.931	1 0 1	2.7	1.7768	1.7774	3 0 0	27.3
4.120	4.117	1 0 2	2.0	1.7666	1.7676	1 1 6	10.6
3.354	3.355	1 0 3	11.6			1 1 $\bar{6}$	0.2
2.777	2.780	1 1 2	3.2	1.7134	1.7112	2 1 4	7.6
		1 1 $\bar{2}$	100.0			2 1 $\bar{4}$	7.3
2.612	2.612	2 0 1	2.1	1.6780	1.6779	2 0 6	1.0
2.464	2.465	2 0 2	0.7	1.6195	1.6193	0 0 8	4.4
2.3305	2.3303	1 0 5	7.1	1.5913	1.5908	2 1 5	0.7
2.2684	2.2687	2 0 3	1.2			2 1 $\bar{5}$	2.3
2.2307	2.2313	1 1 4	24.5	1.5398	1.5392	2 2 0	2.5
		1 1 $\bar{4}$	17.6	1.5912	1.5202	2 0 7	1.8
2.0584	2.0584	2 0 4	1.6	1.4977	1.4975	2 2 2	11.4
2.0010	2.0012	1 0 6	1.7			2 2 $\bar{2}$	0.5
1.9906	1.9916	2 1 1	1.1	1.3996	1.3991	3 1 3	0.3
		2 1 $\bar{1}$	0.1			3 1 $\bar{3}$	1.1
1.8581	1.8581	2 0 5	2.0	1.3904	1.3902	2 2 4	3.0
						2 2 $\bar{4}$	4.2

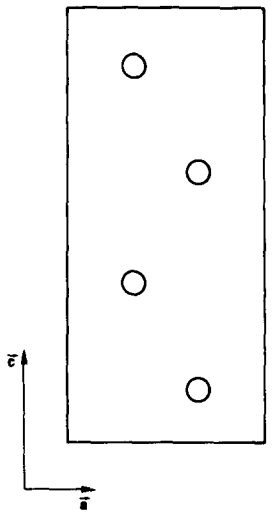

FIG. 1. Sulfur stacking diagram of $Ag_{1/2}In_{1/2}PS_3$ in the a–c side of the unit cell.

TABLE III

POSITIONAL PARAMETERS AND THEIR ESTIMATED STANDARD DEVIATIONS

Atom	x	y	z	B (Å^2)
Ag	$\frac{2}{3}$	$\frac{1}{3}$	$\frac{1}{4}$	4.23(2)
In	0	0	$\frac{1}{4}$	1.247(7)
P	$\frac{1}{3}$	$\frac{2}{3}$	0.1641(1)	0.92(2)
S	0.3145(1)	0.3428(1)	0.11973(6)	1.32(1)

Note. Anisotropically refined atoms are given in the form of the isotropic equivalent thermal parameter defined as $(\frac{4}{3}) * [a^2 \cdot B(1,1) + b^2 \cdot B(2,2) + c^2 \cdot B(3,3) + ab(\cos\gamma) \cdot B(1,2) + ac(\cos\beta) \cdot B(1,3) + bc(\cos\alpha) \cdot B(2,3)]$.

previously assumed from magnetic susceptibility results as far as $Ag_{1/2}Cr_{0.10}In_{0.40}PS_3$ is concerned (*10*). Then, since in the various MPX_3 compounds the (P_2) pairs always present a triangular distribution among the octahedral sites of the so-called filled layers, we expect that it is the case here. It follows that the Ag sublattice also is probably triangular. In addition, and with respect to $FePS_3$ (*12*), the c periodicity implies, as in the copper-containing material, an alternate stacking of ordered cationic a–b planes. As a consequence, and adopting the $P\bar{3}1c$ space group, the atomic positions were taken as follows:

sulfur	in 12*i*,	$x \simeq \frac{1}{3}$,	$y \simeq \frac{1}{3}$,	$z \simeq \frac{1}{8}$;
phosphorous	in 4*f*,	$x = \frac{1}{3}$,	$y = \frac{2}{3}$,	$z \simeq 0.17$;
silver	in 2*d*,	$x = \frac{2}{3}$,	$y = \frac{1}{3}$,	$z = \frac{1}{4}$;
indium	in 2*a*,	$x = 0$,	$y = 0$,	$z = \frac{1}{4}$.

After five series of least-squares cycles with isotropic thermal parameters, the unweighted reliability factor is $R = 0.116$ and the weighted R factor is $R_w = 0.124$ (weights are assigned according to counting statistics). At that stage, the improvement for the refinement was made by introducing anisotropic thermal factors. The R and R_w factors drop to 0.029 and 0.033, respectively, after seven cycles. The final results are $R = 0.028$ and $R_w = 0.031$ by accounting and refining a parameter for isotropic secondary extinction. This parameter is found to be equal to 1.037×10^{-8}. The total number of refined parameters is equal to 18. The

TABLE IV

GENERAL TEMPERATURE FACTOR EXPRESSIONS OF U

Name	$U(1,1)$	$U(2,2)$	$U(3,3)$	$U(1,2)$	$U(1,3)$	$U(2,3)$
Ag	0.0214(2)	$U(1,1)$	0.111(1)	$U(1,1)/2$	0	0
In	0.0101(1)	$U(1,1)$	0.0238(3)	$U(1,1)/2$	0	0
P	0.0087(3)	$U(1,1)$	0.0146(7)	$U(1,1)/2$	0	0
S	0.0188(3)	0.0119(2)	0.0205(3)	0.0084(2)	0.0032(3)	−0.0006(3)

Note. The form of the anisotropic thermal parameter is $\exp[-2\pi^2\{h^2A^2U(1,1) + k^2B^2U(2,2) + l^2C^2U(3,3) + 2hkABU(1,2) + 2hlACU(1,3) + 2klBCU(2,3)\}]$ where A, B, and C are reciprocal lattice constants.

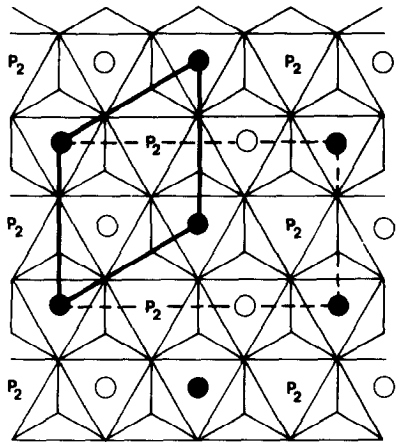

FIG. 2. Ordered distribution of Ag (○), In (●), and P_2 pairs in the a–b planes. The thick line is for edges of the hexagonal cell (this work) and the dashed line is for those corresponding to the previously assumed orthorhombic cell (after (*10*)).

Fourier difference map then calculated was featureless, and refining the occupancy ratio for the heavy atoms does not lead to deviation from the proposed formula.

In Tables III and IV are listed final atomic parameters of the structure and anisotropic temperature factors, respectively. The observed and calculated structure factor table may be sent upon request.

4. Description and Discussion of the Structure

The octahedral sites of the filled layers are occupied in an ordered way (Fig. 2) by indium for one-third of these sites, by silver for the second third, and by phosphorous pairs for the last third. The cationic vacancies are confined to alternate metal layers, forming the so-called van der Waals gap. From one cationic plane to another, the Ag atoms and the (P_2) pairs exchange their positions, resulting in the doubling of the c axis (Fig. 3). The monovalent atom is distributed on a single position within a given octahedral site, in contrast to the two other known $M(I)_{1/2}M(III)_{1/2}PS_3$ compounds (*3*, *4*).

$Ag_{1/2}In_{1/2}PS_3$ is in fact to be compared to $FePSe_3$ (*12*), rather than to $FePS_3$ (*12*). Effectively, as in $FePSe_3$, and as in a few $MPSe_3$ compounds (*13*, *14*), the layered structure is built on an AB sulfur stacking, and not ABC as in $FePS_3$ and as commonly observed for MPS_3. However, for the studied compound, the symmetry is trigonal, when it is rhombohedral in $FePSe_3$ and in a few related selenides (*13*, *14*). In this regard, the structure of $Ag_{1/2}In_{1/2}PS_3$ is unique among the miscellaneous structures of the MPX_3 (X = S, Se) series. More specifically, and as a result of (i) the sulfur stacking nature, (ii) the existence of a van der Waals gap, and (iii) the existence of a threefold axis in the cationic planes, the studied compound is directly related to TiS_2 (CdI_2-type structure (*15*)). Due to cations ordering in the a–b planes and from plane to plane, the a- and c-parameter values of $Ag_{1/2}In_{1/2}PS_3$ are $\sim\sqrt{3}$ and ~ 2 times the a- and c- parameter values of TiS_2, respectively.

In contrast to the (Cu, Cr) and (Ag, Cr) compounds, the metal–sulfur distances among a given site have a unique value. This is due to the fact that Ag(I) and In(III) are isoelectronic and that the [AgS_6] and [InS_6] octahedra have approximately the

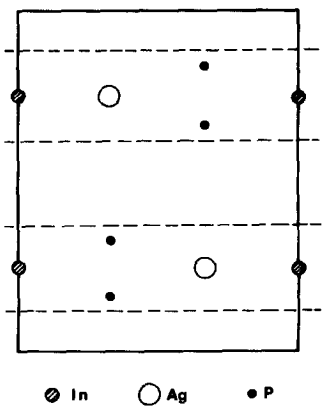

FIG. 3. Section through $(11\bar{2}0)$ planes. The dashed lines are for the projection of the sulfur sheets.

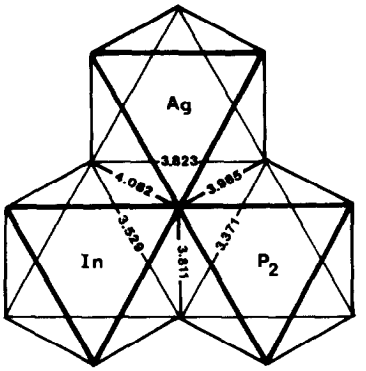

FIG. 4. Different octahedra occurring in the structure of $Ag_{1/2}In_{1/2}PS_3$.

same size, which was not the case for the two mono- and trivalent cation-containing octahedra in the former compounds (*3*, *4*). However, one observes a slight distortion of the sulfur octahedra (they are flattened in the van der Waals gap and elongated in the metal layers) and a small shift of the sulfur position projected along *c* with respect to the ideal positions. The different octahedra occurring in the structure of $Ag_{1/2}In_{1/2}PS_3$ are shown in Fig. 4 and the cation–sulfur distances are given in Table V. The observed values for the Ag–S and In–S distances are in fair agreement with what was expected considering the tabulated cation–sulfur distances by Poix *et al.* (2.78 and 2.61 Å, respectively (*16*)) and also by Tretyakov *et al.* as far as In(III) is concerned (2.63 Å (*17*)).

The P–S distance in the (PS_3) tetrahedra is 2.029 Å, which confirms what has recently been pointed out about such entities in the MPS_3 materials (*18*): the P–S distance does not depend significantly on the nature of *M* and is constant at 2.032 + 0.003 Å. To the contrary, the P–P distance is expected to be correlated to the *M*(II) size (*18*), or average *M*(I)–*M*(III) size as far as the studied compound is concerned. Consequently, in $Ag_{1/2}In_{1/2}PS_3$, knowing that the average metal–sulfur distance (2.71 Å) is close to the Cd–S distance as observed in $CdPS_3$ (2.72 Å, (*18*)), we expect the P–P distance to be approximately the same as in $CdPS_3$ (2.222(2) Å, (*18*)). Effectively, we find d_{P-P} = 2.227(3) Å. As underlined by Brec *et al.*, the (PS_3) groups appear as rigid entities and the P–P distance varies to accommodate the metal size.

TABLE V

CATION–SULFUR DISTANCES (Å)

Ag	In	P
2.778(1)	2.646(1)	2.029(1)
		3.411(1)

Note. Numbers in parentheses are estimated standard deviations.

The last interesting structural feature of the studied compound is the remarkably high value for the isotropic equivalent thermal factor of silver: B_{eq} = 4.23 Å^2. To our knowledge, it is the highest ever encountered in the MPX_3 family (see (*18*)). For example, for Ag in $Ag_{1/2}Cr_{1/2}PS_3$, B_{eq} is much smaller, though comparatively high (2.8 Å^2 (*4*)). Furthermore, as shown by the U_{ij} values for this element (Table IV), the electron cloud related to Ag is very anisotropic and is directed perpendicular to the sheets. From the calculated root-mean-square amplitudes of thermal vibrations (Table VI), the silver electron cloud is estimated to extend, in the *c*-axis direction, over a distance which is twice that corresponding to the other atoms.

TABLE VI

ROOT-MEAN-SQUARE AMPLITUDES OF THERMAL VIBRATION (Å)

Atom	Minimum	Intermediate	Maximum
Ag	0.133	0.179	0.333
In	0.092	0.123	0.154
P	0.085	0.114	0.121
S	0.102	0.128	0.153

TABLE VII

d_I AND d_{III} ARE THE M(I)–S AND M(III)–S OBSERVED AVERAGE DISTANCE (Å), RESPECTIVELY

Compound	d_I	d_{III}	d_I/d_{III}	Sublattice
$Ag_{1/2}Cr_{1/2}PS_3$(4)	2.81	2.43	1.16	Chains
$Cu_{1/2}Cr_{1/2}PS_3$(3)	2.65	2.45	1.08	Triangular
$Ag_{1/2}In_{1/2}PS_3$	2.78	2.65	1.05	Triangular

Note. For the copper-containing compound, d_I represents the average distance between the center of the octahedra and the surrounding sulfur anions.

Such characteristics for the silver electron cloud are probably at the origin of the alternate stacking of Ag atoms and (P_2) pairs along c, owing to steric and repulsive interaction effects.

5. Discussion

We first discuss the origin of the ordered distribution nature in the $M(I)_{1/2}M(III)_{1/2}PS_3$ series. As shown in Table VII, the geometric nature of the metal lattice is correlated to the ratio d_I/d_{III} where d_I and d_{III} are the observed average metal(I)– and metal(III)–sulfur distances. It is thus correlated to the ratio of the sizes of the two kinds of metal-containing octahedra. For smaller ratios, the distribution is triangular (Fig. 2), when for the highest ratio it is so that zigzagging chains are formed (Fig. 5). Such a correlation suggests the following simple explanation.

In $FePS_3$, the (P_2)- and the Fe-containing octahedra are almost the same size (see Fig. 4 in Ref. (*3*)). On substituting the couple $(\frac{1}{2}M(I) + \frac{1}{2}M(III))$ for the divalent metal, the phosphorous pairs sublattice is kept unchanged: one-third of the octahedral sites are occupied by (P_2) and they form a triangular lattice. But, the M(I)- and M(III)-containing octahedra are then distinct at least from the electrostatic point of view since they are changed differently. Treating then the compounds as purely ionic, the coulombic repulsions between the most ionized metals (M^{3+}) will tend to separate these cations. The net repulsive interaction is expected to produce a superlattice in which each cation maximizes the distance to its neighbors (see the Pauling rules and the question of lithium ordering in Li_xTiS_2 from lattice-gas theories (*19, 20*)). Given the number of available octahedral sites in the a–b planes for M^{3+} (one-third), the M^{3+} ions will hence form a triangular lattice in which the $[MS_6]$ nearest neighbors do not share any edge or vertex (Fig. 2). That is also, probably, the reason why the $(P_2)^{8+}$ pairs order into a triangular lattice. Thus, the less charged M^{1+} cations will occupy the remaining octahedral positions (one-third), which also form a triangular lattice.

Such a driving force for cation ordering will hold provided that the M(I)- and M(III)-containing octahedra are approximately the same size, as in $Ag_{1/2}In_{1/2}PS_3$ and $Cu_{1/2}Cr_{1/2}PS_3$. If it is not the case, as in $Ag_{1/2}Cr_{1/2}PS_3$, the coexistence of small cations (e.g., Cr^{3+}) and larger cations (e.g., Ag^+) will lead to important strains and the octahedra will be distorted to accommodate the miscellaneous metal–sulfur distances. Simultaneously, the sulfur anions are sig-

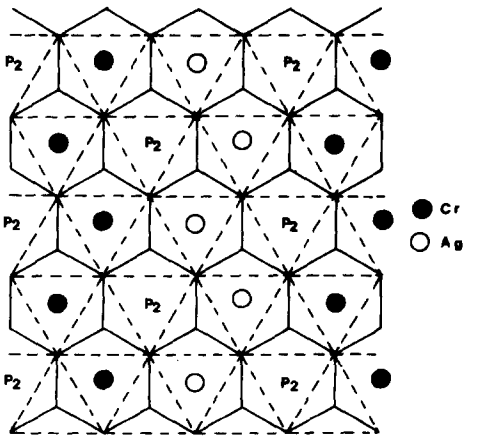

FIG. 5. Chromium and silver zigzagging chains in $Ag_{1/2}Cr_{1/2}PS_3$ (after (*4*)).

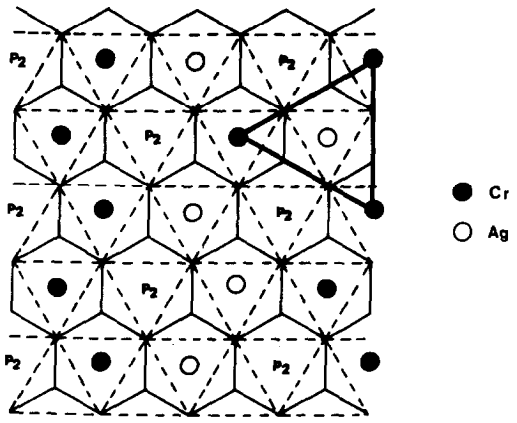

FIG. 6. Schematic local breakdown of the 1D distribution into a triangular one, due to Ag–Cr exchange, in $Ag_{1/2}Cr_{1/2}PS_3$.

nificantly removed from the ideal positions corresponding to an AB or ABC stacking (*4*). The strain energy is thus minimized when the number of shared edges between the smaller and larger octahedra is the smallest. This explains the occurrence of zigzagging chains in $Ag_{1/2}Cr_{1/2}PS_3$: to such a distribution corresponds a single shared edge (Fig. 5), instead of three in the case of a triangular distribution. Note that the breathing of the rigid (PS_3) groups, as discussed in the previous section, then play an important role to locally adjust the anionic lattice from a larger to a smaller neighboring octahedra.

We now discuss the structural and magnetic properties of $Ag_{1/2}Cr_{(1/2-x)}In_xPS_3$. From the above structural results, the In-, and thus the Cr-, sublattice triangular nature is confirmed for $x \gtrsim 0.35$. But, the symmetry is to be considered as trigonal rather than orthorhombic as previously assumed (*10*). So, for higher chromium contents, Ag and (In, Cr) are forming triangular lattices, which means that the repulsive interaction overcomes the steric effects. To the contrary, for smaller chromium contents ($x \lesssim 0.20$), the steric effects overcome the repulsive interaction and the metallic sublattices are characterized by cuts in the zigzagging chains (*10*). However, from the magnitude of the paramagnetic contribution to the total susceptibility for $x = 0$ and 0.01, it has been pointed out that Ag and Cr are partially exchanged and that such an exchange is greatly enhanced by the substitutional-induced disorder (*4, 9*). As a result, part of the chromium is expected to be located out of the chains (Fig. 6). In light of the above discussion, such behavior may be attributed to a local tendency to form a triangular distribution due to an increasing balance between the coulombic and steric effects on increasing the indium content. Knowing that for the trigonal phase ($x \gtrsim 0.35$) the nearest neighbor interactions are ferromagnetic (*10*), the Ag–Cr exchange induces the appearance of new ferromagnetic couplings in the monoclinic phase ($x \lesssim 0.20$). The simultaneous occurrence of antiferromagnetic nearest neighbors and ferromagnetic next-nearest neighbors (Fig. 7) might well be at the origin of the observed spin-glass behavior for the later compounds.

6. Conclusion

In order to test the validity of the proposed driving force for the *M*(I)–*M*(III) distribution nature, we are currently preparing new systems in which the choice of different size *M*(I) and *M*(III) cations would fa-

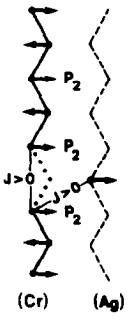

FIG. 7. Ferromagnetic coupling (J) between uncompensated spins for $Ag_{1/2}Cr_{1/2}In_{(1/2-x)}PS_3$ ($x \lesssim 0.20$).

vor either the triangular or the one-dimensional arrangement. In particular, we expect that on substituting Al(III) or Ga(III) for Cr in $Ag_{1/2}Cr_{1/2}PS_3$, the one-dimensional character will be observed from 0 to 100% substitution without cation exchange, since all these trivalent atoms are the same size. In this case, it will be possible to conclude whether or not the ferromagnetic coupling between uncompensated chromium chains within and out of the chains is responsible for a possible spin-glass behavior.

Furthermore, it has been shown by Clement *et al.* that it is possible to substitute M^{2+} cations in the MPS_3 compounds either by alkali or by organometallic cations in aqueous or alcoholic solvent and at moderate temperature (*21, 22*), but not for M = Ni, which presents the lowest thermal factor (*18*). Because of the large thermal factor of Ag in the studied compound (it is the largest so far observed), we expect numerous and easy substitutions of Ag in $Ag_{1/2}In_{1/2}PS_3$, which could lead to various promising phases.

Acknowledgments

The authors thank Professor G. Ferey, Professor R. Brec, Dr. S. Lee, and Dr. P. Grenouilleau for helpful discussions.

References

1. R. BREC, G. OUVRARD, A. LOUISY, AND J. ROUXEL, *Solid State Ionics* **11,** 179 (1983); A. LE MÉHAUTÉ, G. OUVRARD, R. BREC, AND J. ROUXEL, *Mater. Res. Bull.* **12,** 1191 (1977).
2. M. H. WHANGBO, R. BREC, G. OUVRARD, AND J. ROUXEL, *Inorg. Chem.* **24,** 2459 (1985).
3. P. COLOMBET, A. LEBLANC, M. DANOT, AND J. ROUXEL, *J. Solid State Chem.* **41,** 174 (1982).
4. P. COLOMBET, A. LEBLANC, M. DANOT, AND J. ROUXEL, *Nouv. J. Chim.* **7,** 333 (1983).
5. G. LE FLEM, R. BREC, G. OUVRARD, A. LOUISY, AND P. SEGRANSAN, *J. Phys. Chem. Solids* **43,** 455 (1982).
6. P. COLOMBET AND M. DANOT, *Solid State Commun.* **45,** 311 (1983); P. COLOMBET AND L. TRICHET, *Solid State Commun.*, **45,** 317 (1983).
7. Y. MATHEY, H. MERCIER, A. MICHALOWICZ, AND A. LEBLANC, *J. Phys. Chem. Solids* **46,** 1025 (1985).
8. Y. MATHEY, private communication.
9. Z. OUILI, A. LEBLANC, M. DANOT, P. COLOMBET, AND H. MUTKA, *Solid State Commun.* **51,** 259 (1984).
10. A. LEBLANC, Z. OUILI, AND P. COLOMBET, *Mater. Res. Bull.* **20,** 947 (1985).
11. R. YVON, W. JEITSCHKO, AND E. PARTHE, *J. Appl. Cristallogr.* **10,** 73 (1977).
12. W. KLINGEN, R. OTT, AND H. HAHN, *Z. Anorg. Allg. Chem.* **396,** 271 (1973).
13. M. Z. JANDELI, G. EULENBERGER, AND H. HAHN, *Z. Anorg. Allg. Chem.* **447,** 105 (1978).
14. G. OUVRARD, thesis, University of Nantes, France (1980).
15. Y. JEANNIN AND J. BENARD, *C.R. Acad. Sci. Ser. C* **48,** 2875 (1959).
16. P. POIX, F. BASILE, AND C. DJEGA-MARIADASSOUS, *Ann. Chim.* **10,** 159 (1975).
17. YU. D. TRETYAKOV, I. V. GORDEEV, AND YA. A. KESLER, *J. Solid State Chem.* **20,** 345 (1977).
18. R. BREC, G. OUVRARD, AND J. ROUXEL, *Mater. Res. Bull.* **20,** 1257 (1985).
19. M. KABURAGI AND J. KANAMORI, *J. Phys. Soc. Japan* **44,** 718 (1978).
20. R. L. KLEINBERG, R. B. SIBERNAGEL, AND A. H. THOMPSON, *Solid State Commun.* **41,** 401 (1982).
21. R. CLEMENT, *J. Amer. Chem. Soc.* **103,** 6998 (1981).
22. Y. MATHEY, R. CLEMENT, J. P. AUDIERE, O. POIZAT, AND C. SOURISSEAU, *Solid State Ionics* **9** and **10,** 459 (1983).